NON-LINEAR ANALYSIS OF LATERALLY LOADED PILES USING "p-y" CURVES

E. G. Psaroudakis* — MSc Civil Engineer, Department of Civil Engineering, Democritus University of Thrace (DUTh), Greece
Post address: Thermopilon 45, P.K.:54248, Thessaloniki, Greece
E-mail address: empsaroudakis@gmail.com
ORCID: 0000-0002-8540-6127

G. E. Mylonakis — Professor, Chair Geotechnics and Soil-Structure Interaction, University of Bristol, UK
Post address: Queen's Building, University Walk, Clifton BS8 1TR, Bristol, UK
E-mail address: g.mylonakis@bristol.ac.uk
ORCID: 0000-0002-8455-8946

N. S. Klimis — Associate Professor, Department of Civil Engineering, Democritus University of Thrace (DUTh), Greece
Post address: Building B', University Campus of Xanthi - Kimmeria, 67100 Xanthi, Greece
E-mail address: nklimis@civil.duth.gr
ORCID: 0000-0001-9770-2583

*Corresponding author

Keywords: Single pile, Lateral loading, "p-y" curves, Winkler's theory

ABSTRACT: In this paper, we analyze the behavior of a monopile under lateral loading. Specifically, this work focuses on the examination of the static stiffness coefficients of a monopile vertically embedded in a homogeneous or multilayer soil of random geometry and random mechanical properties. To solve the problem, a semi-analytical, closed form solution is developed, based on Winkler's theory. In this model, simulation of the mechanical behavior of the soil is achieved via non-linear "p-y" springs positioned along the axis of the pile, in conjunction with shape functions which describe the lateral movement of the pile. By iterative application of the proposed method the lateral stiffness coefficients at the pile head are calculated with satisfactory accuracy.

The results of the proposed method converge satisfactory enough with real data and other theoretical results coming from sophisticated numerical analysis methods.

1. INTRODUCTION

The most simple and popular approach to the mechanical behavior of laterally loaded piles, is the Winkler model. According to that theory, the interaction between soil and pile takes place via springs placed along the axis of the pile. The force of each spring corresponds to the soil reaction at a specific depth. This model, albeit approximate, is widely used and provides satisfactory results, comparable to more precise methods, such as finite or boundary elements. It has to be noted that lately, a simplified method based on this model was used for the analysis of laterally loaded piles in sloping ground (Pingbao Yin et all, 2018).

The assumption of linear elastic homogeneous soil is often an oversimplification of reality. Conversely, for inhomogeneous profiles it is rather difficult to come up with precise solutions, even when using this simplified theory.

Subsequently, a simple semi-analytical method is developed, based on the Euler-Bernoulli beam model, enhanced by non-linear Winkler springs. The model is used in conjunction with the principle of virtual work and suitable shape functions, which describe the elastic line of a pile under arbitrary force-moment or displacement-rotation pairs at the pile head.

2. PROBLEM DESCRIPTION

The model under examination, consists of a laterally loaded pile of length L, diameter d, modulus of elasticity E_p and maximum bending moment M_y. The pile is considered to be embedded in a homogeneous or multilayer soil of random geometry and random mechanical properties. The soil is characterized by a variable modulus of elasticity $E_s(x)$ and a variable maximum shear strength $p_s(x)$ along with depth (x). At the pile head, a horizontal force P_o and a moment M_o are both applied, as shown in Figure 1. The values of y_o and θ_o, represent the lateral displacement and the rotation of the pile head, respectively.

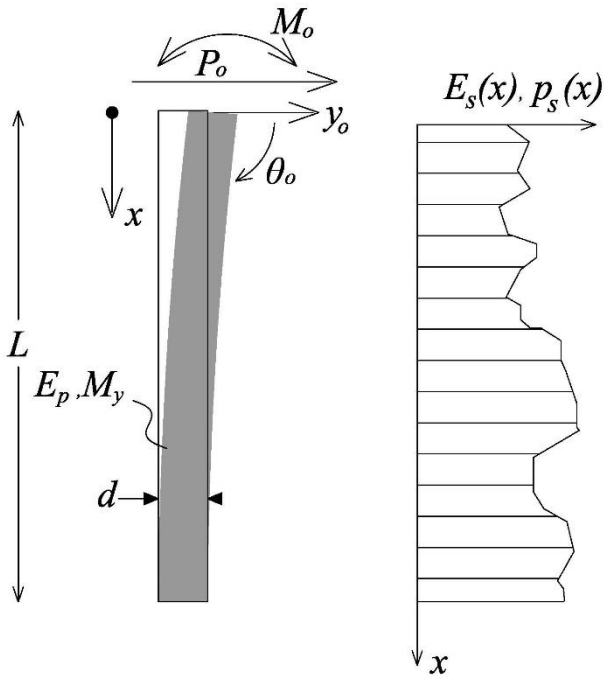

Fig 1. Model of single pile embedded in an inhomogeneous soil

3. DEVELOPMENT OF THE MODEL

3.1 Homogeneous elastic soil

The equation of motion for a laterally loaded single pile on elastic homogeneous foundation, can be easily obtained through equilibrium over a small section of the pile, as presented in figure 2:

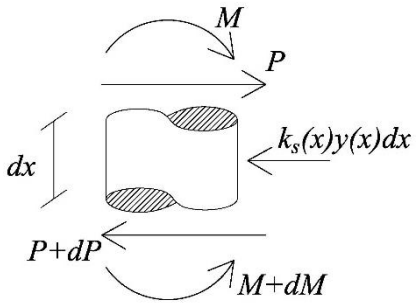

Fig 2. Typical pile segment

According to that, the following eq.1 occurs:

$$P - (P + dP) + k_s(x)dx = 0 \quad (1)$$

Given that:

$$\frac{dP}{dx} = k_s\, y(x) \quad (2)$$

and

$$P = \frac{dM}{dx} \quad (3)$$

we obtain easily the following:

$$\frac{dP}{dx} = \frac{d^2M}{dx^2} = k_s\, y(x) \quad (4)$$

By considering eq. 5:

$$E_p I \frac{d^2y}{dx^2} = -M \quad (5)$$

and double differentiation, we get:

$$E_p I \frac{d^4y}{dx^4} = -\frac{d^2M}{dx^2} \quad (6)$$

by replacing eq. 4 into eq. 6, we obtain:

$$E_p I \frac{d^4y}{dx^4} = -k_s\, y(x) \quad (7)$$

which is the differential equation of a laterally loaded pile:

$$E_p I \frac{d^4y}{dx^4} + k_s\, y(x) = 0 \quad (8)$$

where:

$y(x)$ is the horizontal displacement of the pile at depth x,

k_s is the modulus of Winkler springs (dimensions: force/ square length),

E_p is the modulus of elasticity of the pile's material and

I is the moment of inertia of the pile's section.

Differential eq. 8 can be transformed into eq. 10 by substituting the well known eq. 9 (Hetenyi, 1946):

$$\lambda = \left[\frac{k_s}{4 E_p I} \right]^{1/4} \tag{9}$$

$$\frac{d^4 y(x)}{dx^4} + 4\lambda^4 y(x) = 0 \tag{10}$$

Constant λ has dimensions [1 / length] and is known as Winkler "wavenumber" or "characteristic length". The general solution of eq. 10 is as follows (Hetenyi, 1946):

$$y(x) = e^{\lambda x}\left[A\cos(\lambda x) + B\sin(\lambda x)\right] + e^{-\lambda x}\left[C\cos(\lambda x) + D\sin(\lambda x)\right] \tag{11}$$

where: A, B, C and D represent arbitrary constants depending on boundary conditions, at the base and at the tip of the pile.

Specifically, by setting a unit horizontal displacement at the pile head and zero rotation at the same point, we obtain:

Displacement : $y(0) = 1$ (12a)

Rotation : $y'(0) = 0$ (12b)

Moment : $E_p I_p y''(L) = 0$ (12c)

Shear : $E_p I_p y'''(L) = 0$ (12d)

Solving the 4x4 system of equations 12a-d, bearing in mind that:

$$\sinh \lambda x = \frac{e^{\lambda x} - e^{-\lambda x}}{2} \tag{13}$$

and

$$\cosh \lambda x = \frac{e^{\lambda x} + e^{-\lambda x}}{2} \tag{14}$$

we obtain the values of A, B, C and D:

$$A = \frac{1 + e^{2L\lambda}\left[2 + \cos(2L\lambda) - \sin(2L\lambda)\right]}{1 + e^{4L\lambda} + 2e^{2L\lambda}\left(2 + \cos(2L\lambda)\right)} \tag{15}$$

$$B = \frac{-1 + e^{2L\lambda}\left[\cos(2L\lambda) + \sin(2L\lambda)\right]}{1 + e^{4L\lambda} + 2e^{2L\lambda}\left(2 + \cos(2L\lambda)\right)} \tag{16}$$

$$C = \frac{1}{2}\left(1 + \frac{\sin(2L\lambda) + \sinh(2L\lambda)}{2 + \cos(2L\lambda) + \cosh(2L\lambda)}\right) \tag{17}$$

$$D = \frac{-\cos(2L\lambda) + \cosh(2L\lambda) + \sin(2L\lambda) + \sinh(2L\lambda)}{2\left(2 + \cos(2L\lambda) + \cosh(2L\lambda)\right)} \tag{18}$$

The stiffness matrix, at the pile head, is described below:

$$\begin{Bmatrix} P_o \\ M_o \end{Bmatrix} = \begin{bmatrix} K_{hh} & K_{hr} \\ K_{rh} & K_{rr} \end{bmatrix} \begin{Bmatrix} u_o \\ \theta_o \end{Bmatrix} \tag{19}$$

where: K_{hh}, K_{rr} and K_{hr} (=K_{rh}) are the coefficients in swaying, rocking and cross swaying-crossing respectively. By setting zero rotation and unit displacement at the pile head, according to eq. 19, we obtain:

$$P_o = K_{hh}\, y(0) = K_{hh} u_o \overset{u_o=1}{\Longrightarrow} P_o = K_{hh} \tag{20}$$

and

$$M_o = K_{rh}\, y(0) = K_{rh} u_o \overset{u_o=1}{\Longrightarrow} M_o = K_{rh} \tag{21}$$

substituting eqs 3 and 5 into eqs 20 and 21, the latter are transformed, into:

$$P_o = E_p I \frac{d^3 y(x)}{dx^3} = K_{hh} \tag{22}$$

and

$$M_o = E_p I \frac{d^2 y(x)}{dx^2} = K_{rh} \tag{23}$$

Replacing coefficients A, B, C and D from eqs 15 to 18 into the general solution of eq. 11 and subsequently differentiating two and three times respectively, using eqs 22 and 23, we get:

$$K_{hh} = 4 E_p I \lambda^3 \frac{\sin 2\lambda L + \sinh 2\lambda L}{2 + \cos 2\lambda L + \cosh 2\lambda L} \tag{24}$$

and

$$K_{rh} = 2 E_p I \lambda^2 \frac{-\cos 2\lambda L + \cosh 2\lambda L}{2 + \cos 2\lambda L + \cosh 2\lambda L} \tag{25}$$

In the same way, by setting zero displacement at the pile head and unit rotation at the same point, the following system of equations is obtained:

Displacement : $y(0) = 0$ (26a)

Rotation : $y'(0) = 1$ (26b)

Moment : $E_p I_p y''(L) = 0$ (26c)

Shear : $E_p I_p y'''(L) = 0$ (26d)

Solving again the 4x4 system, we get new values for A, B, C and D:

$$A = \frac{\left[\cos(L\lambda)\right]^2}{\lambda\left(2 + \cos(2L\lambda) + \cosh(2L\lambda)\right)} \tag{27}$$

$$B = \frac{1 + e^{2L\lambda}\left[1 + \sin(2L\lambda)\right]}{\lambda\left(1 + e^{4L\lambda} + 2e^{2L\lambda}\left(2 + \cos(2L\lambda)\right)\right)} \tag{28}$$

$$C = -\frac{\left[\cos(L\lambda)\right]^2}{\lambda\left(2+\cos(2L\lambda)+\cosh(2L\lambda)\right)} \tag{29}$$

$$D = \frac{1+\cosh(2L\lambda)-\sin(2L\lambda)+\sinh(2L\lambda)}{2\lambda\left(2+\cos(2L\lambda)+\cosh(2L\lambda)\right)} \tag{30}$$

As previously, using the stiffness matrix at the pile head (eq. 19) and by imposing zero displacement and unit rotation, we obtain:

$$P_o = K_{hr}\theta_o \overset{\theta_o=1}{\Longrightarrow} P_o = K_{hr} \tag{31}$$

and

$$M_o = K_{rr}\theta_o \overset{\theta_o=1}{\Longrightarrow} M_o = K_{rr} \tag{32}$$

by substituting eqs 3 and 5 into eqs 31 and 33, the latter are transformed into:

$$P_o = E_p I \frac{d^3y(x)}{dx^3} = K_{hr} \tag{33}$$

and

$$M_o = E_p I \frac{d^2y(x)}{dx^2} = K_{rr} \tag{34}$$

The new coefficients, A, B, C and D as obtained from eqs 27 to 30, are introduced into the general solution given by eq. 11 and then. We then, differentiate two and three times respectively the aforementioned equation and by the use of eqs 33 and 34, we finally get:

$$K_{rr} = 2E_p I \lambda \frac{-\sin 2\lambda L + \sinh 2\lambda L}{2+\cos 2\lambda L + \cosh 2\lambda L} \tag{35}$$

$$K_{hr} = 2E_p I \lambda^2 \frac{-\cos 2\lambda L + \cosh 2\lambda L}{2+\cos 2\lambda L + \cosh 2\lambda L} \tag{36}$$

In this way, the stiffness matrix of a monopile of length L (free at the tip), embedded into a homogeneous soil profile, is given by the matrix (Mylonakis, 1995; Mylonakis and Gazetas, 1999):

$$\begin{bmatrix} K_{hh} = 4E_pI\,\lambda^3\frac{\sin 2\lambda L+\sinh 2\lambda L}{2+\cos 2\lambda L+\cosh 2\lambda L} & K_{hr} = K_{rh} = 2E_pI\,\lambda^2\frac{-\cos 2\lambda L+\cosh 2\lambda L}{2+\cos 2\lambda L+\cosh 2\lambda L} \\ K_{rh} = K_{hr} = 2E_pI\,\lambda^2\frac{-\cos 2\lambda L+\cosh 2\lambda L}{2+\cos 2\lambda L+\cosh 2\lambda L} & K_{rr} = 2E_pI\,\lambda\frac{-\sin 2\lambda L+\sinh 2\lambda L}{2+\cos 2\lambda L+\cosh 2\lambda L} \end{bmatrix} \quad (37)$$

3.2 Inhomogeneous elastic soil

The assumption of a linear, elastic and homogeneous soil is definitely an oversimplification of reality. In most cases, the stiffness of soil profiles increases with depth. In this case of an inhomogeneous elastic soil, the eq. 8, which describes the deflection of the pile, is transformed as follows:

$$E_pI\frac{d^4y}{dx^4} + k_s(x)\,y(x)=0 \quad (38)$$

For arbitrary variation of soil stiffness $k_s(x)$ with depth x, a number of solutions have been published using finite and boundary element formulations by Banerjee and Davis (1978), Poulos and Davis (1980), Randolph (1981), etc. Unfortunately, very few analytical solutions exist in the nternational bibliography. In fact, exact solutions have been derived only from Hetenyi (1946), Barber (1953) and Franklin & Scott (1979), for the special case in which stiffness increases linearly with depth, starting from zero value at the free surface. These solutions are power-series of infinite terms, which are not suitable for use in practical problems.

An easy-to-use solution for inhomogeneous elastic soil, of stiffness parabolically increasing with depth, has been proposed by Mylonakis (1995). The type of soil profile considered is presented in Figure 3 and described by equation 39.

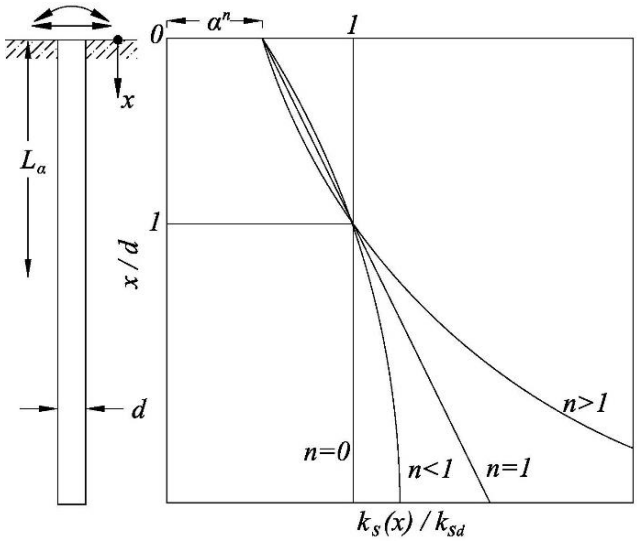

Fig 3. Model of soil stiffness increasing with depth

$$k_s(x) = k_{sd}\left[a + (1-a)\frac{x}{d}\right]^n \tag{39}$$

where:

k_{sd} denotes the value of $k(x)$ at depth of one pile diameter d,

α is a dimensionless parameter of the stiffness coefficient at the soil surface, and

n is a dimensionless shape factor.

The proposed solution (Mylonakis, 1995), is based on replacing the unknown displacement function $y(x)$ (eq. 11), with approximate shape functions $\psi(x)$ and $\varphi(x)$, which describe the lateral displacement of the pile with depth. Specifically, the function $\psi(x)$ describes the displacement of the pile for a unit movement of the head at zero torsion, whereas the $\varphi(x)$ function describes the movement of the pile for unit torsion (1 rad) of the head, at zero displacement, as shown in Figure 4.

By implementation of the aforementioned method, in the case of an inhomogeneous soil profile, we get λ, varying with depth and consequently it is calculated via the following equation:

$$\lambda(x) = \left[\frac{k_s(x)}{4E_pI}\right]^{1/4} \tag{40}$$

Thus, the group of the solutions of eq. 38 can be approximated by eq. 41, based on the general solution of eq. 11:

$$y(x) \cong e^{\lambda(x)x}\left[A\cos(\lambda(x)x)+B\sin(\lambda(x)x)\right]+e^{-\lambda(x)x}\left[C\cos(\lambda(x)x)+D\sin(\lambda(x)x)\right] \quad (41)$$

In order to obtain the shape function $\psi(x)$, constants: A, B, C and D need to be determined, by setting unit horizontal displacement at the pile head and zero rotation at the same point:

Displacement : $y(0)=1$ (42a)

Rotation : $y'(0)=0$ (42b)

Moment : $E_p I_p y''(L)=0$ (42c)

Shear : $E_p I_p y'''(L)=0$ (42d)

Solving the system of equations 42a-d, by bearing in mind equations 13 and 14, we obtain the values of A, B, C and D:

$$A=\frac{1+e^{2L\lambda(x)}\left[2+\cos\left(2L\lambda(x)\right)-\sin\left(2L\lambda(x)\right)\right]}{1+e^{4L\lambda(x)}+2e^{2L\lambda(x)}\left(2+\cos\left(2L\lambda(x)\right)\right)} \quad (43)$$

$$B=\frac{-1+e^{2L\lambda(x)}\left[\cos\left(2L\lambda(x)\right)+\sin\left(2L\lambda(x)\right)\right]}{1+e^{4L\lambda(x)}+2e^{2L\lambda(x)}\left(2+\cos\left(2L\lambda(x)\right)\right)} \quad (44)$$

$$C=\frac{1}{2}\left(1+\frac{\sin\left(2L\lambda(x)\right)+\sinh\left(2L\lambda(x)\right)}{2+\cos\left(2L\lambda(x)\right)+\cosh\left(2L\lambda(x)\right)}\right) \quad (45)$$

$$D=\frac{-\cos\left(2L\lambda(x)\right)+\cosh\left(2L\lambda(x)\right)+\sin\left(2L\lambda(x)\right)+\sinh\left(2L\lambda(x)\right)}{2\left(2+\cos\left(2L\lambda(x)\right)+\cosh\left(2L\lambda(x)\right)\right)} \quad (46)$$

By replacing eqs 43, 44, 45 and 46 into eq. 41, the general solution is transformed into the shape function $\psi(x)$:

$$\psi(x)=\frac{\left[\begin{array}{l} e^{-\lambda(x)(2L+x)}(e^{2L\lambda(x)}(1+e^{2\lambda(x)x})\cos\lambda(x)(2L-\lambda(x))+ \\ +(2e^{2L\lambda(x)}+e^{4L\lambda(x)}+e^{2\lambda(x)x}+2e^{2\lambda(x)(L+x)})\cos\lambda(x)x- \\ -e^{2L\lambda(x)}(-1+e^{2\lambda(x)x})\sin\mu(2L-x)+ \\ +(e^{4L\lambda(x)}-e^{2\lambda(x)x})\sin\lambda(x)x) \end{array}\right]}{2(2+\cos 2L\lambda(x)+\cosh 2L\lambda(x))} \quad (47)$$

In the same way, by imposing a unit rotation (1 rad) at the pile head at zero displacement, we obtain:

Displacement : $y(0)=0$ (48a)

Rotation : $y'(0)=1$ (48b)

Moment : $E_pI_py''(L)=0$ (48c)

Shear : $E_pI_py'''(L)=0$ (48d)

and subsequently, we get new values for constants A, B, C and D:

$$A=\frac{\left[\cos(L\lambda(x))\right]^2}{\lambda(x)(2+\cos(2L\lambda(x))+\cosh(2L\lambda(x)))} \quad (49)$$

$$B=\frac{1+e^{2L\lambda(x)}\left[1+\sin(2L\lambda(x))\right]}{\lambda(x)(1+e^{4L\lambda(x)}+2e^{2L\lambda(x)}(2+\cos(2L\lambda(x))))} \quad (50)$$

$$C=-\frac{\left[\cos(L\lambda(x))\right]^2}{\lambda(x)(2+\cos(2L\lambda(x))+\cosh(2L\lambda(x)))} \quad (51)$$

$$D=\frac{1+\cosh(2L\lambda(x))-\sin(2L\lambda(x))+\sinh(2L\lambda(x))}{2\lambda(x)(2+\cos(2L\lambda(x))+\cosh(2L\lambda(x)))} \quad (52)$$

By replacing again, eqs 49, 50, 51 and 52 into eq. 41, the shape function $\varphi(x)$ is structured as following:

$$\varphi(x)=\frac{\left[\begin{array}{l} 2\cosh L\lambda(x)\ \cosh\lambda(x)(L-x)\ \sin\lambda(x)x+ \\ +(\cos\lambda(x)(2L-x)+\cos\lambda(x)x)\sinh\lambda(x)x \end{array}\right]}{\lambda(x)(2+\cos 2L\lambda(x)+\cosh 2L\lambda(x))} \quad (53)$$

Both of the above shape functions ($\psi(x)$, $\varphi(x)$) correspond to a floating pile with zero moment and shear at the tip.

Replacing $\lambda(x)$ by μ, defined as "shape" parameter equal to the average value of $\lambda(x)$ along the "active" length, (L_a) of the pile, we obtain:

$$\mu = \frac{1}{L_a} \int_{x=0}^{L_a} \lambda(x)\, dx \tag{54}$$

Parameter μ in a homogeneous soil is equal to the wavenumber λ (eq. 9). In non-homogeneous soil profiles, μ is approximated by the mean value of λ within an "active" length (L_a) of the pile (eq. 55). "Active" length (L_a) is defined as the length beyond which the pile behaves as a semi-infinite long beam (Poulos & Davis, 1980; Randolph, 1981). That is, any increase of the pile length beyond L_a, does not affect the stiffness at the pile head. Usually "active" length is of the order of 10 to15 pile diameters (Velez et al., 1983). There have been many expressions for L_a in various types of soil profiles (Randolph, 1981; Gazetas,1991;). In the present case the "active" length is calculated by an iterative process using eqs 55 and 56.

$$L_a = \chi\, d \left[\frac{E_p}{\overline{E_s}} \right]^n \tag{55}$$

$$\overline{E_s} = \frac{1}{L_a} \int_{x=0}^{L_a} E_s(x)\, dx \tag{56}$$

starting from a reasonable initial hypothesis e.g. $L_a = 10d$. The active length of the pile depends mostly on the ratio (E_p / E_s). Recommended values for parameters χ and n are presented in Table 1.

Table1. Recommendations for parameters χ and n for inhomogeneous soil layers

Reference	Inhomogeneous soil profile	
	χ	n
Davies & Budhu (1986)	1.3	0.22

Gazetas (1991)	2.0	0.2
Fleming et al. (1993)	2.2	0.25
Syngros (2004)	2.5	0.2

The total displacement of a pile, can be calculated by the sum of the products of each unit function multiplied by the horizontal movement (u_o) and rotation (θ_o) at the pile head:

$$y(x) = u_o\psi(x) + \theta_o\varphi(x) \quad (57)$$

Assuming that a theoretical approximate function – solution *g(x)*, describes the lateral displacement of the pile, this function should satisfy the following conditions:

- be at least thrice differentiable
- fulfil the boundary conditions

Multiplying eq. 38 by this approximate function – solution *g(x)* and then integrating along the pile, we get equation (58):

$$\int_0^L E_pI\frac{d^4y}{dx^4}g(x)dx + \int_0^L k_s(x)\,y(x)\,g(x)dx = 0 \quad (58)$$

Integrating by parts the first term of the latter equation, it is transformed into a simpler form:

$$\int_0^L E_pI\left(\frac{d^3y}{dx^3}\right)'g(x)dx + \int_0^L k_s(x)\,y(x)\,g(x)dx = 0 \Rightarrow \quad (59)$$

$$E_pI\frac{d^3y}{dx^3}g(x)\Big|_{x=0}^{x=L} - \int_0^L E_pI\frac{d^3y}{dx^3}g'(x)dx + \int_0^L k_s(x)\,y(x)\,g(x)\,dx = 0 \Rightarrow \quad (60)$$

$$E_pI\frac{d^3y}{dx^3}g(x)\Big|_{x=0}^{x=L} - \int_0^L E_pI\left(\frac{d^2y}{dx^2}\right)'g'(x)dx + \int_0^L k_s(x)\,y(x)\,g(x)\,dx = 0 \Rightarrow \quad (61)$$

$$E_pI\frac{d^3y}{dx^3}g(x)\Big|_{x=0}^{x=L} - E_pI\frac{d^2y}{dx^2}g'(x)\Big|_{x=0}^{x=L} + \int_0^L E_pI\frac{d^2y}{dx^2}g''^{(x)}dx +$$
$$+ \int_0^L k_s(x)\,y(x)\,g(x)\,dx = 0 \Rightarrow \quad (62)$$

Provided that shear and moment across the pile are given by equations:

$$E_p I \frac{d^3 y}{dx^3} = Q(x) \tag{63}$$

and

$$E_p I \frac{d^2 y}{dx^2} = Q(x) \tag{64}$$

we replace the above equations into eq. 62 and thus, we get:

$$Q(x)g(x)|_{x=0}^{x=L} - M(x)g'(x)|_{x=0}^{x=L} + \int_0^L E_p I \frac{d^2 y}{dx^2} g''(x)dx + \tag{65}$$
$$+ \int_0^L k_s(x)y(x)\, g(x)dx = 0 \Rightarrow$$

$$[Q(L)g(L) - Q(0)g(0)] - [M(L)g'(L) - M(0)g'(0)] + \tag{66}$$
$$+ \int_0^L E_p I \frac{d^2 y}{dx^2} g''(x)dx + \int_0^L k_s(x)y(x)\, g(x)dx = 0 \Rightarrow$$

$$Q(L)g(L) - Q(0)g(0) - M(L)g'(L) + M(0)g'(0) + \tag{67}$$
$$+ \int_0^L E_p I \frac{d^2 y}{dx^2} g''(x)dx + \int_0^L k_s(x)y(x)\, g(x)dx = 0 \Rightarrow$$

Bearing in mind that moment and shear at the pile tip are equal to zero and that at the pile head $M(0)=M_o$ and $Q(0)=Q_o$, we get:

$$-Q_o g(0) + M_o g'(0) + \int_0^L E_p I y''(x) g''(x)dx + \int_0^L k_s(x)y(x)\, g(x)dx = 0 \tag{68}$$

Now, assuming that $g(x)$ is equal to $y(x)$:

$$g(x) = y(x) = u_o \psi(x) \tag{69}$$

and setting unit displacement at the pile head ($g(0)=y(0)=1$) and zero rotation at the same spot ($g'(0)=y'(0)=0$), eq. 68 is transformed into equation 70:

$$Q_o u_o = \int_0^L E_p I u_o \psi''(x) u_o \psi''(x) dx + \int_0^L k_s(x) u_o \psi(x) u_o \, \psi(x) dx \Rightarrow \quad (70)$$

$$Q_o u_o = {u_o}^2 \left[\int_0^L E_p I \psi''(x) \psi''(x) dx + \int_0^L k_s(x) \psi(x) \, \psi(x) dx \right] \Rightarrow \quad (71)$$

$$Q_o = u_o \underbrace{\left[\int_0^L E_p I \psi''(x) \psi''(x) dx + \int_0^L k_s(x) \psi(x) \, \psi(x) dx \right]}_{K_{hh}} \Rightarrow \quad (72)$$

$$K_{hh} = E_p I \int_0^L [\psi''(x)]^2 dx + \int_0^L k_s(x) [\psi(x)]^2 \, dx \quad (73)$$

In the same way, by imposing zero displacement at the pile head ($g(0)=y(0)=0$) and a unit rotation ($g'(0)=y'(0)=1$), assuming again that $g(x)$ is equal to $y(x)$:

$$g(x) = y(x) = \theta_o \varphi(x) \quad (74)$$

eq. 68 is transformed into:

$$-M_o \theta_o = \int_0^L E_p I {\theta_o}^2 [\varphi''(x)]^2 dx + \int_0^L k_s(x) \, {\theta_o}^2 [\varphi(x)]^2 dx \Rightarrow \quad (75)$$

$$-M_o \theta_o = {\theta_o}^2 \left[\int_0^L E_p I [\varphi''(x)]^2 dx + \int_0^L k_s(x) \, [\varphi(x)]^2 dx \right] \Rightarrow \quad (76)$$

$$-M_o = \theta_o \underbrace{\left[\int_0^L E_p I [\varphi''(x)]^2 dx + \int_0^L k_s(x) \, [\varphi(x)]^2 dx \right]}_{K_{rr}} \Rightarrow \quad (77)$$

$$K_{rr} = \int_0^L E_p I [\varphi''(x)]^2 dx + \int_0^L k_s(x) \, [\varphi(x)]^2 dx \quad (78)$$

Finally, by replacing $y(x)=u_o\psi(x)$ and $g(x)=\theta_o\varphi(x)$ and considering a unit displacement at the pile head ($u_o=1$) while setting free the rotation (θ_o), simulating thus a free head pile under lateral load, eq. 68 is transformed into:

$$Q_o u_o - M_o \theta_o = \int_0^L E_p I u_o \psi''(x) \theta_o \varphi''(x) dx +$$

$$+ \int_0^L k_s(x) u_o \psi(x) \theta_o \, \varphi(x) dx \xrightarrow{u_o=1} \quad (79)$$

$$Q_o - M_o\theta_o = \int_0^L E_p I\psi''(x)\theta_o\varphi''(x)dx + \int_0^L k_s(x)\psi(x)\theta_o\,\varphi(x)dx \Rightarrow \quad (80)$$

Due to free head boundary condition, as far as the rotation is concerned, $M_o=0$:

$$Q_o = \theta_o \underbrace{\int_0^L E_p I\psi''(x)\varphi''(x)dx + \int_0^L k_s(x)\psi(x)\,\varphi(x)dx}_{K_{hr}} \Rightarrow \quad (81)$$

$$K_{hr} = \int_0^L E_p I\psi''(x)\varphi''(x)dx + \int_0^L k_s(x)\psi(x)\,\varphi(x)dx \quad (82)$$

Also, because of the symmetric matrix, we get $K_{hr}=K_{rh}$

Using the aforementioned stiffness parameters, the following expression is obtained which describes the piles waying, rocking and cross swaying-rocking head stiffness of a floating pile (Mylonakis, 1995):

$$K_{ij} = E_p I \int_0^L \chi_i''(x)\chi_j''(x)dx + \int_0^L k_s(x)\chi_i(x)\,\chi_j(x)dx \quad (83)$$

The two terms in the right-hand side of eq.86 stand for the contributions to the overall stiffness of the pile. The first term of the same equation stands for the pile flexural stiffness, whilst the second, for the soil stiffness.

The two subscripts i and j refer to swaying and rocking stiffness respectively. When $\chi_i(x)=\chi_j(x)=\psi(x)$ the swaying stiffness K_{hh} is obtained. When $\chi_i(x)=\chi_j(x)=\varphi(x)$ the rocking stiffness K_{rr} is obtained. Finally, when $\chi_i(x)=\psi(x)$ and $\chi_j(x)=\varphi(x)$ the cross swaying-rocking stiffness K_{hr}(=K_{rh}) is calculated.

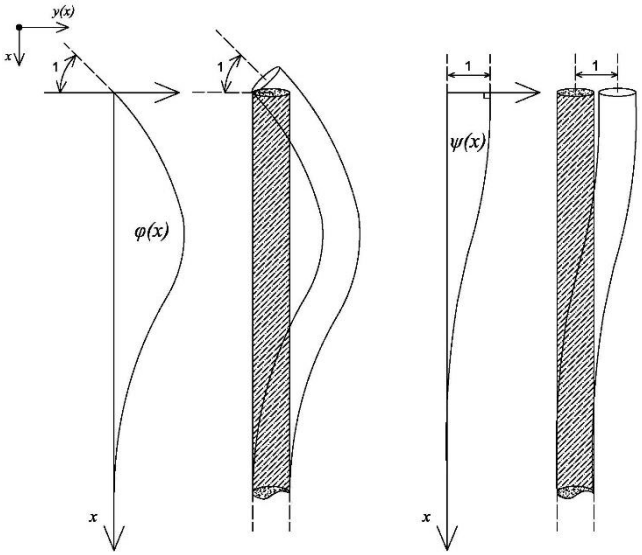

Fig 4. Shape functions *φ(x)* and *ψ(x)*

4. NON-LINEARITIES OF THE PROBLEM

The problem of the laterally loaded monopile, involves two main non-linearities. The first refers to soil behavior, while the second refers to the behavior of the pile material.

4.1 Soil non-linearity

To simulate soil behavior, at small lateral displacements, the “p-y” curves are used. These curves were derived experimentally by analyzing load tests on piles, mainly by McClelland & Focht (1958), Matlock (1970), Reese and Van Impe (2001), and Cox et al. (1974). A typical curve is shown in Figure 5. The initial part of the curve consists of a small segment which describes the behavior of soil micro-movements (elastic behavior) and its stiffness is defined as δE_s, where δ is a dimensionless constant ranging between 1 and 1.5 (Novak et al., 1978; Roesset, 1980; Scott, 1981; Dobry et al., 1982), and E_s, is the modulus of elasticity of the soil at a specific depth. The final (horizontal) part of the curve defines the maximum response of the soil in large horizontal displacements (p_{max}), and is calculated based on limit equilibrium analysis. The slope and the shape of the curve depends on the depth (near the pile head or in greater depth), the soil type (clay, sand, soft rock), the loading conditions (monotonic or cyclic) and the diameter of the pile.

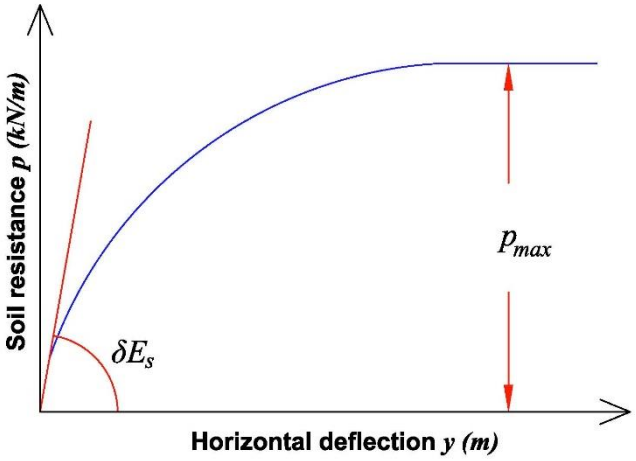

Fig 5. Typical *"p-y"* curve

4.2 Pile non-linearity

The second source of nonlinearity is detected in the behavior of the pile material. Based on materials theory, the secant stiffness (E_pI) of the pile section is reduced as the bending moment applied increases. To understand this phenomenon, a typical moment-curvature diagram is presented in Figure 6. In the following trilinear moment-curvature diagram, there are three points that define the flexural behaviour of the cross section: (A) Concrete crack, (B) Yield of tensile steel rods (C) Section collapse.

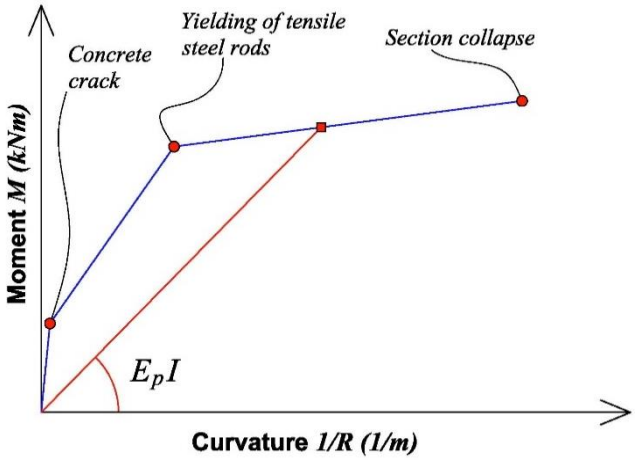

Fig 6. Typical moment curvature diagram of concrete pile section

5. DEVELOPMENT OF NON-LINEAR SOLUTION

For the development of a nonlinear model, Mylonakis solution (1995) was used incorporated with "p-y" springs, describing soil non-linearity and moment-curvature

diagram, representing the stiffness of the pile material. Based on the stiffness matrix at the head of the pile (eq. 19) and throughout trial and error iterative process, by adjusting each of the two non-linearities (soil non-linearity through “p-y” curves, through M-1/R diagram) convergence is reached (Psaroudakis, 2013). The eleven steps of the process are presented one by one, below:

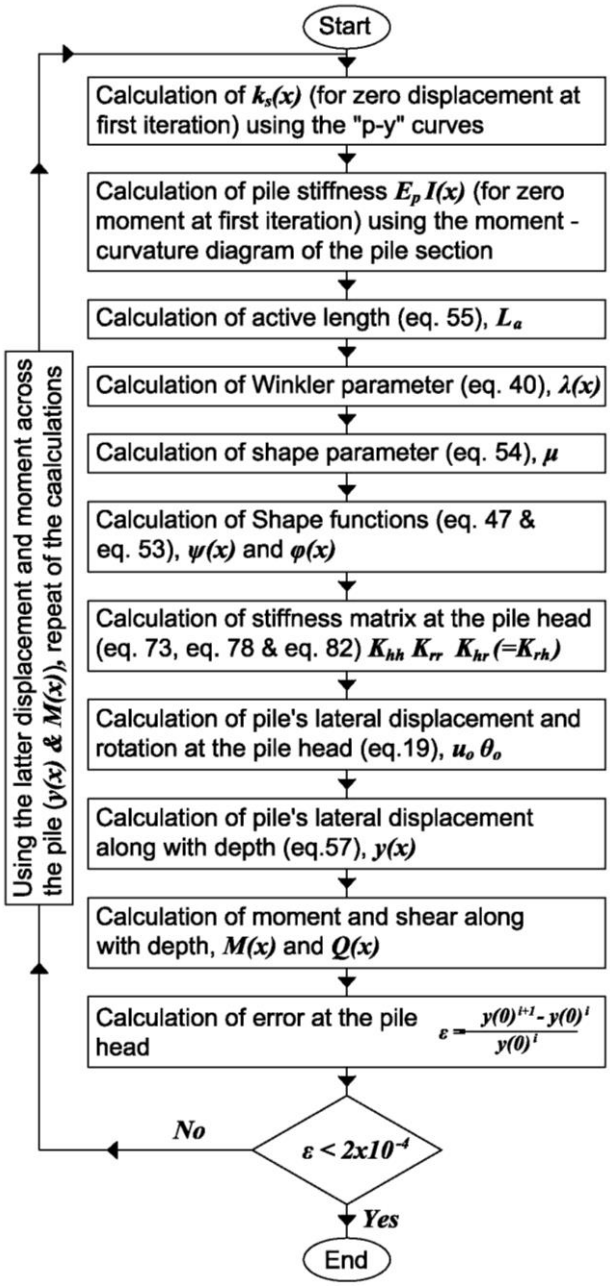

Fig 7. Flowchart of iterative process

The aforementioned “algorithm”, in case of inhomogeneous soil, converges in less than 15 loops and remains stable even for lateral loads close to failure.

6. RELIABILITY OF THE PROPOSED METHOD

Hereafter are presented three case studies where theoretical results from the proposed method are compared to real field data from in-situ pile load tests.

6.1 Case study No 1

A monotonic lateral pile load test took place in 2005 for the construction of a bridge at Aliakmon River, Greece (Comodromos and Pitilakis, 2005).The pile was of length $L=52m$, diameter $d=1.0m$, made of concrete C30/35 and steel bars S500 (in longitudinal direction16Φ25).The soil layers are shown in Table 2 and during the test, the groundwater table was located at the ground surface. The horizontal load was applied through a hydraulic jack which was placed at the surface level.

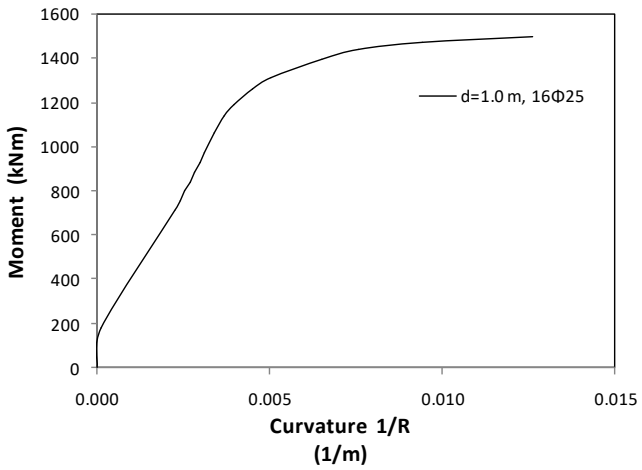

Fig 8. Moment curvature diagram of diameter $d=1.0m$ circular pile, calculated by software Response-2000

Table2. Stratigraphy and geotechnical parameters used in 1st example

Layer	Soil Type	Soil Characteristics	Top-Bottom
Layer 1	Soft clay (CL)	G=90c_u, c_u=5-50kPa, φ'=0°, γ=20.0kN/m^3	0.0-36.0m
Layer 2	Hard clay (CL)	K=8.33MPa, G=3.35MPa, c_u=110kPa, γ=20kN/m^3, φ'=0°, γ=20.0kN/m^3	36.0-48.0m
Layer 3	Thick gravel (GW)	K=40MPa, G=24MPa, φ'=40°, γ=22.0kN/m^3, k=50.0MN/m^3	48.0-52.0m

φ'	: Friction angle (deg)
γ	: Eff. unit weight (kN/m^3)
k	: Lat. Subgrade modulus (MN/m^3)
c_u	: Undrained shear strength (kPa)
G	: Shear modulus (MPa)

K	: Bulk modulus (MPa)
E_s	: Modulus of elasticity (MPa)
q_u	: Unconfined compressive strength (kPa)

After the completion of the field test, numerical analyses were followed using the software FLAC3D (finite difference software by ITASCA, 2005), COM623 (finite difference software; Sullivan,1977) and EPile (software implementing the proposed solution with the use of Davies & Budhu parameters χ and n, for the calculation of "active" length (Psaroudakis, 2013). For the analysis, the pile's section nonlinearity was implemented through moment-curvature diagram presented above (Figure 8) and the soil non-linearity through "p-y" curves (Reese and Van Impe, 2001). The results of the analyses are presented in force-displacement (at the pile head) diagrams, normalized by the marginal load (Broms, 1964a-b; $P_B \approx 803.0kN$) and the diameter (d) of the pile. In Figure 9 the analysis results for elastic pile and non-linear soil are depicted, whereas in Figure10 the analysis results for both non-linear pile and soil behavior are also presented. Additionally, in these diagrams the ultimate lateral resistance of the pile is presented, calculated via the method proposed by Loukidis and Vavourakis (2014). The latter method estimates the pile limit lateral resistance in elastic-perfectly plastic soil under plane strain conditions. An equation, based on FE analysis results, is used for the estimation of limit lateral pile resistance, in non-dilative cohesionless and cohesive frictional soils.

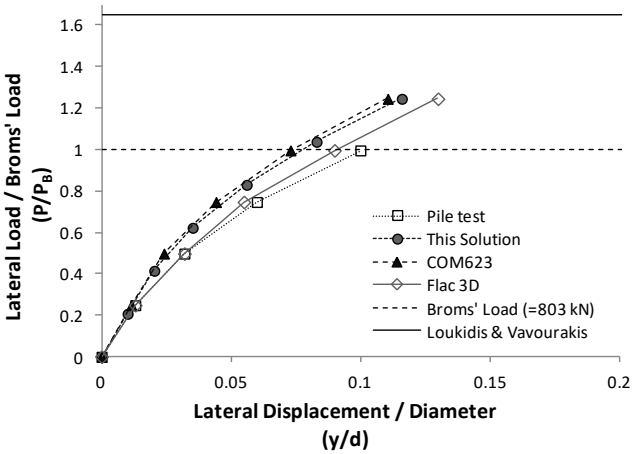

Fig 9. Force - displacement normalized diagram, on the head of an elastic pile

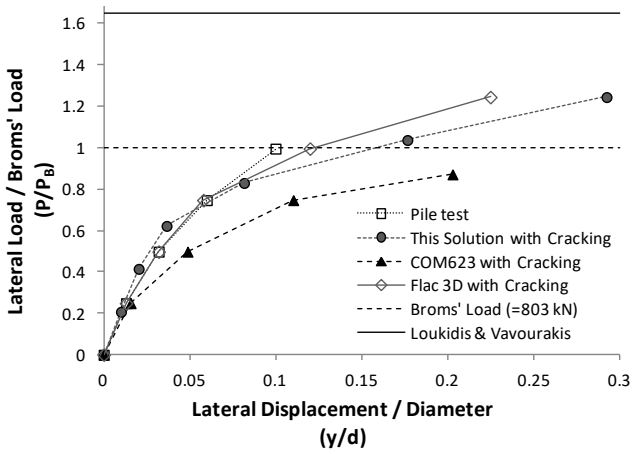

Fig 10. Force - displacement normalized diagram, on the head of an inelastic pile

6.2 Case study No 2

The 2nd pile test was carried out at the area located between the harbour of Thessaloniki (Northern Greece) and the intersection of the main motorway and the ring road, 10km southwest of city center (Comodromos et al, 2009). Likewise, the previous example, the groundwater table was located at the ground surface. The stratigraphy of the area is presented in Table 3. The pile was of length $L=32m$, diameter $d=0.8m$ and was made of concrete C20/25 and steel bars S500 (longitudinal direction 16Φ18).

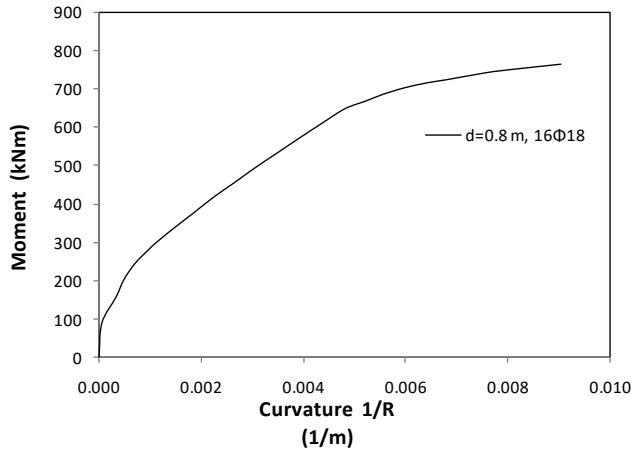

Fig 11. Moment curvature diagram of diameter $d=0.80m$ circular pile, calculated by software SOFISTIK

Table3. Stratigraphy and geotechnical parameters used in 2nd example

Layer	Soil Type	Soil Characteristics	Top-Bottom

Layer 1	Loose Sand (SM/ML)	φ'=30°, γ=20.0kN/m^3,E_s=25.0MPa,c'=3.0kPa, k=30.0MN/m^3	0.0-6.0m
Layer 2	Dense Sand (SM/ML)	φ'=35°, γ=20.0kN/m^3,E_s=35.0MPa,c'=5.0kPa, k=40.0MN/m^3	6.0-12.0m
Layer 3	Soft Clay (OH)	q_u=30-50kPa, γ=17.0kN/m^3, c'=25±10kPa, φ'=5±5°, E_s=30.0MPa	12.0-25.0m
Layer 4	Hard Clay (CL)	q_u=170±70kPa, γ=21.0kN/m^3, c'=110±20kPa, φ'=0-5°, E_s=80.0MPa	25.0-35.0m

φ'	: Friction Angle (deg)
c'	: Cohesion (kPa)
γ	: Effective unit weight (kN/m^3)
k	: Lateral subgrade modulus (MN/m^3)
E_s	: Modulus of elasticity (MPa)
q_u	: Unconfined compressive strength (kPa)

The numerical simulation of the pile load test was performed using the finite difference code COM623 (Sullivan, 1977) and EPile (with the use of Davies &Budhu parameters χ and n; Psaroudakis, 2013). In Figure 11 the moment-curvature diagram of the section is presented, used for the non-linear analysis, whilst the soil response is simulated through "p-y" springs (Reese and Van Impe, 2001). The results of the analyses are presented in force-displacement (at the pile head) diagrams, normalized to the marginal load (Broms 1964a-b; $P_B \approx 459.0kN$) and the diameter (d) of the pile. In Figure 12 the analysis results for elastic pile and non-linear soil are depicted, whereas in Figure 13 the analysis results for both non-linear pile and soil behavior are presented. In the aforementioned diagrams is also presented the limit lateral resistance of the pile, calculated via the method proposed by Loukidis and Vavourakis (2014).

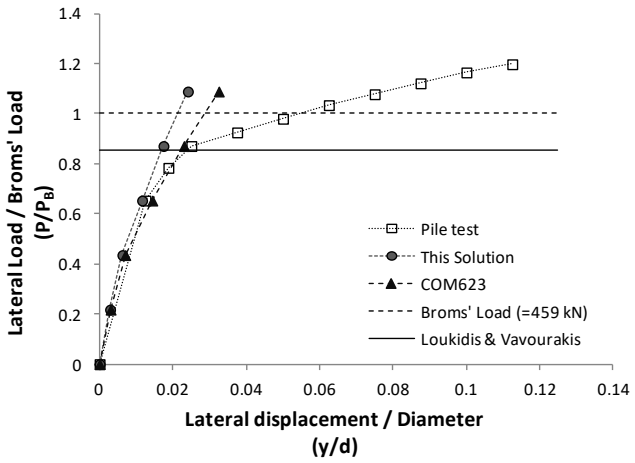

Fig 12. Force - displacement normalized diagram, on the head of an elastic pile

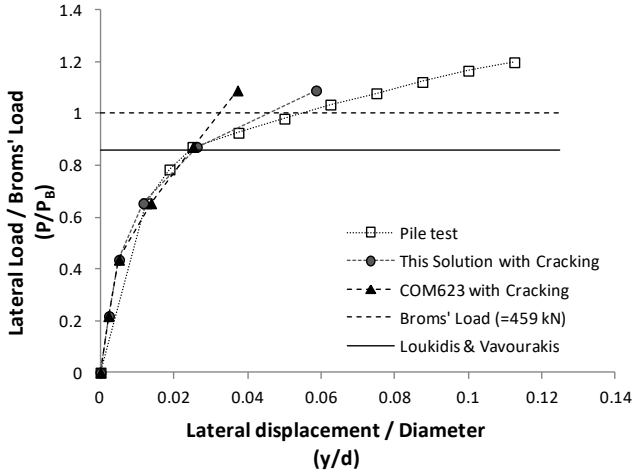

Fig 13. Force -displacement normalized diagram, on the head of an inelastic pile

6.3 Case study No 3

This pile test took place on Treasure Island in San Francisco Bay, California. Although the testing program was designed to evaluate the lateral load behavior of piles and pile groups in liquefied sand produced by controlled blasting, the lateral behavior of the piles, prior to liquefaction was also determined for comparison purposes (Rollins et al., 2005). The groundwater table was found at a depth of 0.5m below the ground surface. The pile was a $0.324m$ outside diameter, A252 Grade 3 steel pipe with $9.5mm$ wall thickness and length equal to $L\approx11.5m$. The moment of inertia of the section was $I=1.16\times10^{-4}\ m^4$. However, an angle iron was attached to opposite sides of the pile in the direction of loading to protect the strain gages, which increased the moment of inertia to $I=1.43\times10^{-4}\ m^4$, modifying the stiffness of the section to $E_pI\approx28.600\ kNm^2$. The horizontal load was applied at a height of $0.69m$ above the ground surface, through a hydraulic pump.

Table 4. Stratigraphy and geotechnical parameters used in 3rd example according to API (1987)

Layer	Soil Type	Soil Characteristics	Top-Bottom
Layer 1	Sand (SP)	φ'=33°, γ=19.50kN/m³,c'=0kPa, k=24.4MN/m³	0.0-0.51m
Layer 2	Sand (SP-SM)	φ'=33°, γ=10.3kN/m³,c'=0kPa, k=15.4MN/m³	0.51-2.59m
Layer 3	Sand (SP-SM)	φ'=32°, γ=10.3kN/m³,c'=0kPa, k=13.6MN/m³	2.59-4.73m
Layer 4	Sand (SM)	φ'=30°, γ=10.3kN/m³,c'=0kPa, k=10.8MN/m³	4.73-7.49m
Layer 5	Soft Clay (CL)	φ'=0°, γ=9.5kN/m³,e_{50}=0.01,c'=19.2kPa	7.49-9.25m

Layer 6	Sand (SP)	φ'=30°, γ=10.3kN/m^3,c'=5.0kPa, k=10.8MN/m^3	9.25-10.16m
Layer 7	Soft Clay (CL)	φ'=0°, γ=9.5kN/m^3,e_{50}=0.01,c'=19.2kPa	10.16-11.84m

φ'	: Friction Angle (deg)
c'	: Cohesion (kPa)
γ	: Effective unit weight (kN/m^3)
k	: Lateral subgrade modulus (MN/m^3)
e_{50}	: Strain corresponding to one-half of the compressive strength of clay

The numerical simulation of the pile test was performed using the software LPile Plus v.3.0 (Finite difference code, Reese et al.,1997), SWM v.3.2 (Finite difference code, Ashour et al., 2002) and EPile (Psaroudakis, 2013).The results of the analyses are presented in force-displacement (at the pile head) diagrams, normalized to the marginal load (Broms 1964a-b; $P_B \approx 113.5kN$) and the diameter (d) of the pile. For the geotechnical site characterization, a number of in situ tests were performed (SPT, CPT, etc.). For the present case study, two soil profiles are available (Bolton, 1986; API, 1987) and are respectively presented in Tables 4 and 5.

Table 5. Stratigraphy and geotechnical parameters used in 3rd example according to Bolton (1986)

Layer	Soil Type	Soil Characteristics	Top-Bottom
Layer 1	Sand (SP)	φ'=39°(38°), γ=19.50kN/m^3,c'=0kPa, k=60.0MN/m^3	0.0-0.51m
Layer 2	Sand (SP-SM)	φ'=39°(38°), γ=10.3kN/m^3,c'=0kPa, k=35.2MN/m^3	0.51-2.97m
Layer 3	Sand (SP-SM)	φ'=37°(36°), γ=10.3kN/m^3,c'=0kPa, k=29.8MN/m^3	2.97-3.99m
Layer 4	Sand (SP-SM)	φ'=36°(33°),γ=10.3kN/m^3,c'=0kPa, k=24.4MN/m^3	3.99-6.00m
Layer 5	Sand (SM)	φ'=35°(34°),γ=10.3kN/m^3,c'=0kPa, k=21.7MN/m^3	6.00-7.49m
Layer 6	Soft Clay (CL)	φ'=0°, γ=9.5kN/m^3,e_{50}=0.01,c'=19.2kPa	7.49-9.25m
Layer 7	Sand (SP)	φ'=34°(33°),γ=10.3kN/m^3,c'=5.0kPa, k=19.0MN/m^3	9.25-10.16m
Layer 8	Soft Clay (CL)	φ'=0°, γ=9.5kN/m^3,e_{50}=0.01,c'=19.2kPa	10.16-11.84m

φ'	: Friction Angle (deg)
c'	: Cohesion (kPa)
γ	: Effective unit weight (kN/m^3)
k	: Lateral subgrade modulus (MN/m^3)
e_{50}	: Strain corresponding to one-half of the compressive strength of clay

*In parenthesis is the friction angle used for the analysis with SWM

Figures 14 and 15 present the results from this pile test, as well as the analysis results by the three software (EPile, SWM and LPile) according to API and Bolton correlations

respectively. From the analysis coming from EPile software, it is concluded that the best convergence of theoretical results with the pile test, was achieved with the combined use of parameters χ and n, according to Gazetas (1991) and API profile (see Table 4). Additionally, in these diagrams the limit lateral resistance of the pile is also presented, calculated using both methods proposed by Broms (1964a-b) and Loukidis & Vavourakis (2014). Non-linear pile behavior was not taken into account in this case study.

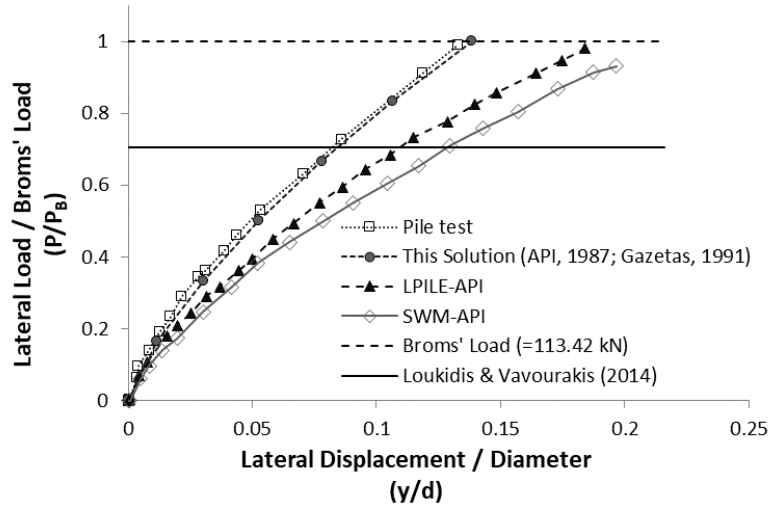

Fig 14. Force - displacement normalized diagram, on the head of an elastic pile, based on API profile

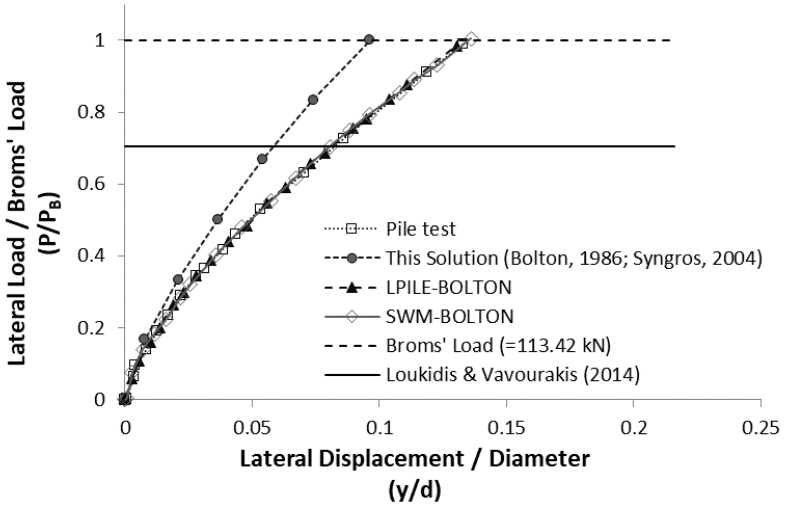

Fig 15. Force - displacement normalized diagram, on the head of an elastic pile, based on Bolton's profile

In all three examples (case studies), the results of the proposed solution are in good agreement with the experimental measurements. Specifically, it is obvious that the analysis of both non-linear pile and non-linear soil follows closely the results of the pile

test contrary to the one in which only the soil is considered as non-linear. The analysis with COM623 (elastic pile, finite difference analysis) shows greater deviation even for low load values. In the third example, the calculation is performed for elastic pile behavior, whilst the results of the method, using API correlation seems to be closer to the real field data. In the first example, Loukidis and Vavourakis (2014) method overestimates the limit lateral resistance of the pile compared to Broms method, whereas in the second example seems to be more conservative and accurate than Broms. This explains the reason why Loukidis and Vavourakis (2014) method is proposed mostly for limit lateral pile resistance estimation in cohesionless soils.

7. PRACTICAL APPLICATION OF THE PROPOSED METHOD

Unlike numerical solutions, which demand discretization of the pile into finite elements and afterwards, resolution of a system of complicated linear equations, the proposed innovative method, requires only discretization of the pile into "cells", in order to integrate with depth, using a simple worksheet. The results of the method are considered satisfactory, as they converge fairly well with those coming from more rigorous methods based on complicated numerical analyses. The practical application of the method is based on its simplicity and accuracy and it is considered ideal for aquick, yet reliable evaluation of experimental data and results from numerical analyses.

8. CONCLUSIONS

1. A numerical model has been developed, for the analysis of non–linear problem of a laterally loaded single pile avoiding use of finite elements or finite differences and consequently resolution of numerous linear systems.
2. The method calculates displacement and rotation directly based on the shape functions, while shear stresses and moments are calculated by consecutive integrations of soil deflection along the pile.
3. Since the proposed method is not based on matrix inversion, it is extremely stable even for loads close to failure.
4. If soil is simulated by linear springs, then the proposed solution is entirely identical to the already existing solutions in bibliography. In the case of a

homogeneous soil, convergence is achieved without iterative process, while in the case of inhomogeneous soil, convergence is usually achieved in less than ten (10) iterations.

5. The suggested method has also been compared to real field data, in three cases (USA & Greece), with a noticeable success.
6. Due to the combined advantages, such as, stability, accuracy, economy and ease of use, it is our belief that the proposed method can be reliably applied for the evaluation of experimental data and results from numerical analyses.

REFERENCES

[1] American Petroleum Institute (1987) Recommended Practice for Planning, Designing and Constructing Fixed Offshore Platforms. API Recommended Practice, 2A (RP 2A), 17th Ed.

[2] Ashour M., Norris G. and Pilling P. (2002), Strain Wedge Model Capability of Analyzing Behavior of Lateral Loaded Isolated Piles, Drilled Shafts and Pile Groups. Journal of Bridge Engineering, Vol. 7, No. 4, pp. 245-254

[3] Banerjee P.K., Davis T.G. (1978), The behavior of axially and laterally loaded single piles embedded in non-homogeneous soils. Géotechnique, Vol. 28, No. 3, pp. 309-326

[4] Barber E.S. (1953), Discussion to Paper by SM Gleser. ASTM, SPT 154, pp. 96-99

[5] Bolton M.D .(1986), The Strength and Dilatancy of Sands. Géotechnique, Vol. 36, No. 1, pp. 65-78

[6] Broms B.B. (1964a), Lateral Resistance of Piles in Cohesive Soils. Proceedings of the American Society of Civil Engineers, Journal of the Soil Mechanics and Foundations Division, Vol. 90, SM2

[7] Broms B.B. (1964b), Lateral Resistance of Piles in Cohesionless Soils. Proceedings of the American Society of Civil Engineers, Journal of the Soil Mechanics and Foundations Division, Vol. 90, SM3

[8] Comodromos E.M. and Pitilakis K.D. (2005), Response Evaluation for Horizontally Loaded Fixed-Head Pile Groups Using 3-D Non-Linear Analysis. International Journal for Numerical and Analytical Methods in Geomechanics, Vol. 29, No. 6, pp. 597-625

[9] Comodromos E.M., Papadopoulou M.C. and Rentzeperis I.K. (2009), Pile Foundation Analysis and Design using Experimental Data and 3D Numerical Analysis. Computers and Geotechnics, Vol. 36, No.5, pp. 819-836

[10] Cox W.R., Reese L.C. and Grubbs B.R. (1974), Field Testing of Laterally Loaded Piles in Sand. Proceedings of the 6th Annual Offshore Technology Conference, Huston, Texas, pp. 459-487

[11] Davies T.G., Budhu M. (1986), Nonlinear Analysis of Loaded Piles in Heavily Overconsolidated clays. Géotechnique, Vol. 36, No. 4, pp. 527-538

[12] Dobry R., O'Rourke J.M., Roesset M.J. and Vicente E. (1982), Stiffness and damping of single piles. Journal of Geotechnical Engineering, Division 108, pp. 439-459

[13] Franklin J.F. and Scott R.F. (1979), Beam Equation with Variable Foundation Coefficient. J. Eng. Mech., ASCE, 105, 5, pp. 811-827

[14] Gazetas G. (1991), Foundation Vibrations. Foundation Engineering Handbook. 2nd Edition, HY Fang, ed., Van Nostrand Reinholds, Chapter 15, pp. 553-593

[15] Hetenyi M. (1946) Beams on Elastic Foundations. Univ. of Michigan Press: Michigan

[16] ITASCA Consulting Group: FLAC3D (2005) Fast Lagrangian Analysis of Continua. Minneapolis

[17] Loukidis D. and Vavourakis V. (2014), Limit Lateral Resistance of Vertical Piles in Plane Strain. 8th European Conference on Numerical Methods in Geotechnical Engineering, pp. 681-685

[18] Matloc H. (1970), Correlation for Design of Laterally Loaded Piles in Soft Clay. Proceedings of the 2nd Offshore Technology Conference. Dallas, Texas, pp. 577-594

[19] McClelland B. and Focht J. (1958), Soil Modulus for Laterally Loaded Piles. Transactions of the American Society of Civil Engineers. Vol. 123, pp 1049-1086

[20] Mylonakis G. (1995), Contributions to the Static and Seismic Analysis of Piles and Pile-Supported Bridge Piers. PhD Dissertation, State University of New York

[21] Mylonakis G., and Gazetas G. (1999), Lateral Vibration and Internal Forces of Grouped Piles in Layered Soil. Journal of Geotechnical and Geoenviromental Engineering, ASCE, Vol. 125, No. 1, pp. 1-10

[22] Novak M., Nogami T. and Aboul-Ella F. (1978), Dynamic soil reaction for plane-strain case. Journal of Engineering Mechanics, ASCE, Vol. 104, No. 4, pp. 953-959

[23] Pingbao Yin, Wei He and Zhaohui Joey Yang (2018), A Simplified Nonlinear Method for a Laterally Loaded Pile in Sloping Ground. Advances in Civil Engineering, Vol. 2018, ID. 5438618

[24] Poulos H.G. and Davis E.H. (1980), Pile Foundation Analysis and Design. John Willey & Sons

[25] Psaroudakis E. (2013), Non-Linear Analysis of Laterally Loaded Piles Using "p-y" Curves. MSc Dissertation, University of Patras

[26] Randolph M.F. (1981), The Response of Flexible Piles to Lateral Loading. Géotechnique, Vol. 31, No. 2, pp. 247-259

[27] Reese L.C. and Van Impe W.F. (2001), Single Piles and Pile Groups under Lateral Loading. Balkema, Rotterdam, The Netherlands

[28] Reese L.C., Wang S.T., Arrellaga J.A. and Hendrix J. (1997), LPile Plus 3.0 for Windows, Ensoft Ink., Austin, Texas

[29] Response-2000 (2001) Reinforced Concrete Sectional Analysis using the Modified Compression Field Theory. Evan Bentz at Department of Civil Engineering, University of Toronto, Canada, V.0.8.5

[30] Roesset J.M. (1980), Stiffness and damping coefficients of foundations. Proc. ASCE Geotechnical Engineering Division National Convention, pp. 1-30

[31] Rollins K.M., Lane J.D. and Gerber T.M. (2005), Measured and Computed Lateral Response of a Pile Group in Sand. Journal of Geotechnical and Geoenviromental Engineering, Vol. 131, No. 1, pp. 103-114

[32] Scott R.F. (1981), Foundation Analysis. Prentice Hall, Englewood Cliffs

[33] Sullivan W.R. (1977), Development and evaluation of a unified method for the analysis of laterally loaded piles in clay. Unpublished MSc Dissertation, University of Texas, Austin

[34] Syngros C. (2004), Seismic Response of Piles and Pile-Supported Bridge Piers Evaluated Through Case Histories. PhD Dissertation, The City College and the Graduate Center of the City University of New York

[35] Velez A., Gazetas G. and Krishnan R. (1983), Static and dynamic lateral deflection of piles in non-homogeneous soil stratum. Géotechnique, Vol. 33, No. 3, pp. 307-325